Original Article

Linear Accuracy of Cone Beam CT Derived 3D Images

April A. Brown[a]; William C. Scarfe[b]; James P. Scheetz[c]; Anibal M. Silveira[d]; Allan G. Farman[b]

ABSTRACT

Objective: To compare the in vitro reliability and accuracy of linear measurements between cephalometric landmarks on cone beam computed tomography (CBCT) 3D volumetric images with varying basis projection images to direct measurements on human skulls.

Materials and Methods: Sixteen linear dimensions between 24 anatomic sites marked on 19 human skulls were directly measured. The skulls were imaged with CBCT (i-CAT, Imaging Sciences International, Hatfield, Pa) at three settings: (a) 153 projections, (b) 306 projections, and (c) 612 projections. The mean absolute error and modality mean ($\pm$ SD) of linear measurements between landmarks on volumetric renderings were compared to the anatomic truth using repeated measures general linear model ($P \leq .05$).

Results: No difference in mean absolute error between the scan settings was found for almost all measurements. The average skull absolute error between marked reference points was less than the distances between unmarked reference sites. CBCT resulted in lower measurements for nine dimensions (mean difference range: 3.1 mm $\pm$ 0.12 mm to 0.56 mm $\pm$ 0.07 mm) and a greater measurement for one dimension (mean difference 3.3 mm $\pm$ 0.12 mm). No differences were detected between CBCT scan sequences.

Conclusions: CBCT measurements were consistent between scan sequences and for direct measurements between marked reference points. Reducing the number of projections for 3D reconstruction did not lead to reduced dimensional accuracy and potentially provides reduced patient radiation exposure. Because the fiducial landmarks on the skulls were not radio-opaque, the inaccuracies found in measurement could be due to the methods applied rather than to innate inaccuracies in the CBCT scan reconstructions or 3D software employed. (*Angle Orthod.* 2009; 79:150–157.)

KEY WORDS: Cephalometry; Computed tomography; Cone beam; Radiography; Cephalometric

INTRODUCTION

Over the past decade, cone beam computed tomography (CBCT), specifically for imaging the maxillofacial region, has been developed. CBCT images provide useful datasets to generate both two-dimensional (2D) planar projection[1–4] and three-dimensional (3D) surface or volume rendered images[5,6] for use in orthodontic assessment and treatment planning.

CBCT can provide submillimeter spatial resolution for images of the craniofacial complex with scanning times comparable to panoramic radiography and generally at lower radiation dosages than ascribed to fan-beam or helical CT imaging methods[7,8] and a similar order of magnitude to other dental radiographic modalities.[9–11] This possibility, and the increasing access of CBCT imaging in orthodontics, is a component of the paradigm that is directing imaging analysis from 2D cephalometry to 3D visualization of craniofacial morphology.[12]

The cone-beam technique uses rotational scanning of an x-ray source and reciprocating x-ray detector around the patient's head to produce multiple single projection images. These images are similar to lateral "cephalometric" radiographic images, each slightly off-

[a] MS in Oral Biology candidate, Graduate School, University of Louisville School of Dentistry, Louisville, Ky.

[b] Professor, Department of Surgical/Hospital Dentistry, University of Louisville School of Dentistry, Louisville, Ky.

[c] Professor, Department of Diagnostic Sciences, Prosthetic and Restorative Dentistry, University of Louisville School of Dentistry, Louisville, Ky.

[d] Professor, Department of Orthodontic and Pediatric Dentistry, University of Louisville School of Dentistry, Louisville, Ky.

Corresponding author: Dr William Charles Scarfe, Department of Surgical/Hospital Dentistry, University of Louisville School of Dentistry, 501 South Preston St, Louisville, KY 40292 (e-mail: wcscar01@gwise.louisville.edu)

Accepted: March 2008. Submitted: December 2007.

DOI: 10.2319/122407-599.1

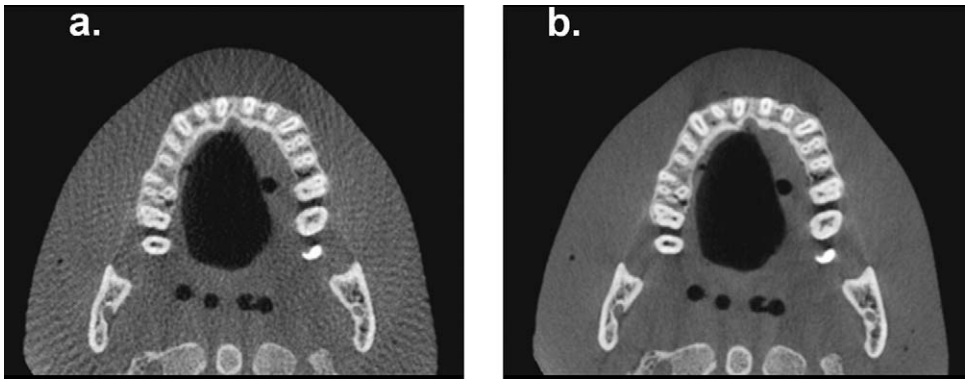

Figure 1. Axial orthogonal image of phantom demonstrating the effect of image quality of increasing the number of projections used to construct a volumetric dataset from (a) 306 projections (20s scan) to (b) 612 projections (40s scan).

set from one another. The complete series of images is referred to as the projection data. The number of images comprising the projection data is determined by the frame rate (number of images acquired per second), the completeness of the trajectory arc, and the speed of the rotation. The number of projection scans comprising a single scan may be fixed (eg, Newtom 3G, QR Inc, Verona, Italy; Iluma, Imtec Inc, Ardmore, Okla; Galileos, Sirona AG, Bensheim, Germany, or Promax 3D, Planmeca Oy, Helsinki, Finland) or variable (eg, i-CAT, Imaging Sciences International, Hatfield, Pa; PreXion 3D, TeraRecon Inc, San Mateo, Calif).

More projection data provide more information to reconstruct the image, allow for greater spatial and contrast resolution, increase the signal-to-noise ratio producing "smoother" images, and reduce metallic artifacts. However, this usually is accomplished with a longer scan time, a higher patient dose, and longer primary reconstruction time. Reducing the number of projections used to reconstruct the volumetric database may reduce patient radiation exposure but results in altered image quality (Figure 1). As CBCT technology is being applied to 3D orthodontic imaging, the use of techniques to minimize patient exposure and their effect on cephalometric analysis accuracy should be investigated.

The effect of reducing the number of projections used to reconstruct renderings for use in 3D cephalometric analysis has not been previously reported. Therefore, this study was undertaken to compare the in vitro reliability and accuracy of linear measurements between cephalometric landmarks from CBCT derived 3D surface renderings from variable numbers of projection images.

MATERIALS AND METHODS

This observational cross-sectional in vitro experiment was approved by the Institutional Human Remains Committee at our university. The sample consisted of 19 dry dentate human skulls with a stable and reproducible occlusion, presence of a full permanent dentition, and similar skull size. Fifteen craniometric landmarks, of which nine were bilateral (Table 1), were identified on each skull using an indelible marker providing 24 anatomic sites. Landmarks were chosen to provide representative linear dimensions in vertical, transverse, and horizontal planes. Operational definitions were developed as elaborations or modifications of those presented by previous authors.[13,14] The dimensions between specific points provided 16 linear distances commonly used in cephalometric orthodontic analysis (Figure 2). To establish the true distances between the selected anatomic points, measurements were made by the principal investigator and a research associate three times independently using an electronic digital caliper (27-500-90, GAC, Bohemia, NY). The mean of the measurements served as anatomic truth.

To provide soft tissue equivalent attenuation, two latex balloons filled with water were placed in the cranial vault prior to imaging. To separate the mandibular condyle from the temporal fossa, a 1.5-mm thick Styrofoam wedge was placed in the joint space between the glenoid fossa and the condylar head. For all images, the teeth were placed in centric occlusion (maximum intercuspation). A custom plastic head holder was constructed to support the skulls during imaging. The anterior symphyseal region of the mandible of each skull was inserted into the chin holder and vertical and horizontal lasers were used to position the skull. The specimen was oriented by adjustment of the chin support until the midsagittal plane was perpendicular to the floor and the horizontal laser reference coincided with the intersection of the posterior maxillary teeth and alveolar ridge.

Cone beam CT images were acquired using a maxillofacial CBCT unit capable of a full head scan (i-CAT

Table 1. Definition of Craniometric Surface Landmarks Used in the Cephalometric Analysis

Landmark	Abbreviation	Definition
Midline		
Nasion	Na	A midsagittal point on the bridge of the nose at the most superior point of frontonasal suture
Anterior nasal spine	ANS	Most anterior limit of the floor of the nose, at the tip of the anterior nasal spine in the midsagittal plane
A point	A	The deepest (most posterior) on the anterior curvature of the maxilla in the midsagittal plane
Posterior nasal spine	PNS	The most posterior extent of the hard palate in the midsagittal plane
B point	B	The deepest (most posterior) point on the anterior curvature of the mandible in the midsagittal plane
Menton	Me	Most inferior point along the curvature of the chin in the midsagittal plane
Bilateral		
Medio-orbitale	Mo	The point on the medial orbital margin that is the most distal point along the frontomaxillary suture
Lateral piriform aperture	NC	The most lateral aspect of the piriform aperture
Antegonion	Ag	The most superior point in the antegonial notch
Gonion	Go	A point on the inferior surface of the mandible which lies midway along the curvature between the ramus and the body.
Zygomatic arch	Za	A point at the most lateral surface of the zygomatic arch near the zygomaticomaxillary suture
Condylion	Co	The most superior point of the condylar head
Zygomaticofrontal medial suture point	Z	The point at the medial margin of the orbital rim at the zygomaticofrontal suture
Mental foramen	Mf	The most distolateral point of the mental foramen on the buccal surface of the mandible
Jugale; maxillare	J	The most inferior point in the curvature of the lateral contour of the maxillary alveolar process

Classic, Imaging Sciences International). Full trajectory (360°) rotational scans were acquired for each skull with a 17.0 cm (diameter) × 13.2 cm (height) field of view at 0.4 mm voxel resolution. Three scan settings were used producing volumetric datasets comprised of different numbers of basis projections. (a) CBCT 10: 10 second, 153 projections; (b) CBCT 20: 20 second, 306 projections; and (c) CBCT 40: 40 second, 612 projections. Primary and secondary reconstruction of the data was automatically performed immediately after acquisition.

The CBCT data were imported in DICOM multifile format into Dolphin 3D (V.10, Dolphin Imaging, Chatsworth, Calif) on the same computer. All reconstructions and measurements were performed on a 20.1-inch flat panel color monitor (FlexScan L888, Eizo Nanao Technologies Inc, Cypress, Calif) screen with a resolution of 1600 × 1200 at 85 Hz and a 0.255 mm dot pitch, operated at 24 bit. This software is capable of generating 3D shaded surface display volumetric rendered images using the entire volumetric data set. This involves generating an image of the skull by manually adjusting the threshold of visible pixel levels, a process called segmentation (Figure 3). This provided 3D renderings which demonstrated visual differences, depending on the number of projection images used in the reconstruction (Figure 4). Next, the 3D image was reoriented such that the Frankfort horizontal plane was parallel to the lower border of the screen display in both sagittal and coronal projections. Then, the cephalometric landmarks were located and marked on the image. The Dolphin 3D software enabled measurements to be performed from different views using rotation and translation of the rendered image. This was performed by a sequence of preset volumetric orientations.

Finally, measurements between specific landmarks were made. A custom analysis within the program was developed that directed the observer to identify specific anatomic landmarks on the images using a cursor-driven pointer. For the version of the software version used, points and planes were unnamed. Therefore, it was necessary to select points to identify a linear plane. This was performed in a specific sequence such that linear measurements corresponded to particular cephalometric planes and were calculated by the proprietary measurement algorithm. In this way linear measurements could be exported directly as text data. This procedure was repeated three times by the principal author.

The text data were exported into a database (Microsoft Excel 2007, Microsoft, Redmond, Wash). The mean and standard deviation of three repeats of the measurements performed by consensus was calculated for each skull and used as anatomic truth. For each imaging mode, the average of three triplicate indepen-

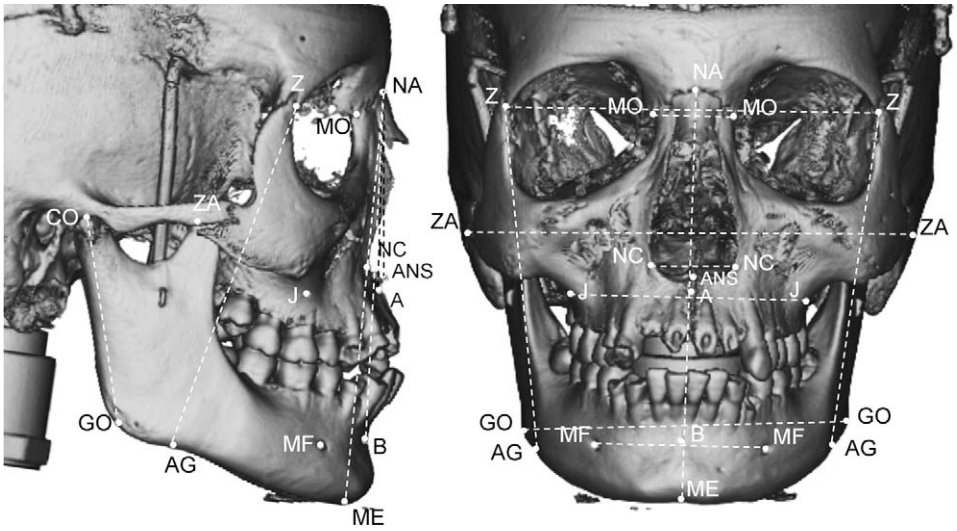

Figure 2. Anatomic landmarks / planes used in the analysis are shown on lateral (left, lt) and frontal (right, rt) projections of 3D shaded surface rendering. Linear distances were determined for the following dimensions: Na-Me = nasion–menton; Co-Go (lt and rt side) = condylion–gonion; Z-Ag (lt and rt side) = zygomaticofrontal medial suture point–antegonion; Na-ANS = nasion–anterior nasal spine; ANS-PNS = anterior nasal spine–posterior nasal spine; Na-A = nasion–A point; Na-B = nasion–B point; Go-Go = gonion (rt)–gonion (lt); Mf-Mf = mental foramen (rt)–mental foramen (lt); Mo-Mo = medio-orbitale (rt)–medio-oribitale (lt); Za-Za = zygomatic arch (rt)–zygomatic arch (Lt); NC-NC = nasal canal (rt)–nasal canal (lt); Z-Z = zygomaticofrontal medial suture point (rt)–zygomaticofrontal medial suture point (lt); J-J = jugale (rt)–jugale (lt).

dent analyses from the principle investigator was used. The data files were coded for use with statistical software (SPSS V.12, Chicago, Ill). To determine intraobserver reliability, absolute mean error (± SD) was calculated for triplicate measurements. Mean measurements within modality groups were compared with the repeated measure general linear model using the Wilks lambda multivariate test ($P \leq .05$) and the Sidak adjustment for multiple comparisons.

RESULTS

Table 2 shows the mean absolute intrarater measurement error for 3D CBCT and skull measurements. Overall mean percentage measurement error for anatomic skull dimensions (0.45 mm ± 0.17 mm; range: 0.1 mm ± 0.08 mm to 0.75 mm ± 0.71 mm) was significantly lower than the error for CBCT 10 ($P < .001$; mean difference = 0.44 mm), CBCT 20 ($P < .001$; mean difference = 0.38 mm), and CBCT 40 ($P < .001$; mean difference = 0.32 mm). There were no differences between CBCT modalities. For 10 of the 16 measurements at least one of the CBCT mean absolute errors was significantly higher than direct skull measurements.

Table 3 provides comparison of mean linear measurements obtained from each 3D CBCT reconstruction and actual skull dimensions. For six dimensions, there were no differences between 3D CBCT and actual skull measurements. All CBCT scan settings produced lower measurements than skull values for six dimensions (Na-Me, Z-$Ag_{rt/lt}$, ANS-PNS, Za-Za, NC-NC) (mean difference 3.1 mm ± 0.12 mm). For Na-ANS and Z-Z, CBCT 20/40 dimensions were less than skull measurements (mean difference 0.56 mm ± 0.07 mm) whereas for Mf-Mf CBCT 10/40 dimensions were less than skull measurements (mean difference 2.96 mm ± 0.18 mm). For Mo-Mo, CBCT measurements were greater than actual skull measurement (mean difference 3.4 mm ± 0.12 mm).

DISCUSSION

Maxillofacial cone beam imaging provides clinicians with an opportunity to generate 3D volumetric renderings using relatively inexpensive third party personal computer based software. The availability of this technology will undoubtedly expand the use and application of 3D imaging in the field of orthodontics. However, while CBCT provides this facility at doses substantially lower than conventional CT, patient radiation dose is still several times higher than conventional cephalometric and panoramic digital imaging modalities. Appropriate selection of exposure settings (eg, kVp, mAs) and adjustment of additional technical parameters are recommended to provide protocols aimed at minimizing patient dose. The aim of this study was to compare the reliability and accuracy of linear dimensions between common cephalometric landmarks on a sample of skulls to 3D measurements obtained from shaded surface 3D renderings reconstructed from CBCT datasets obtained from varying numbers of projection images.

While the reliability of measurements taken directly

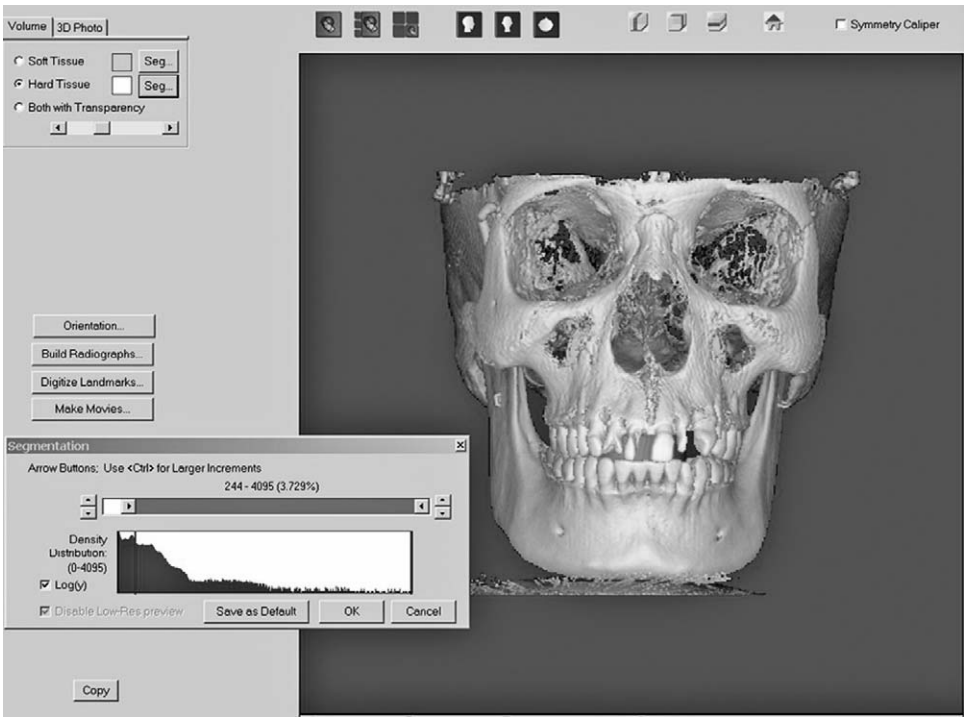

Figure 3. Screen capture from Dolphin 3D program demonstrating the segmentation process. The hard tissue volume segmentation is selected (upper left) and using the segmentation cursor (lower left), the displayed gray level of the voxels is dynamically altered to provide the most realistic appearance of the skull with minimal loss of cortical bone due to thin structures and minimal superimposition of artifacts and soft tissue.

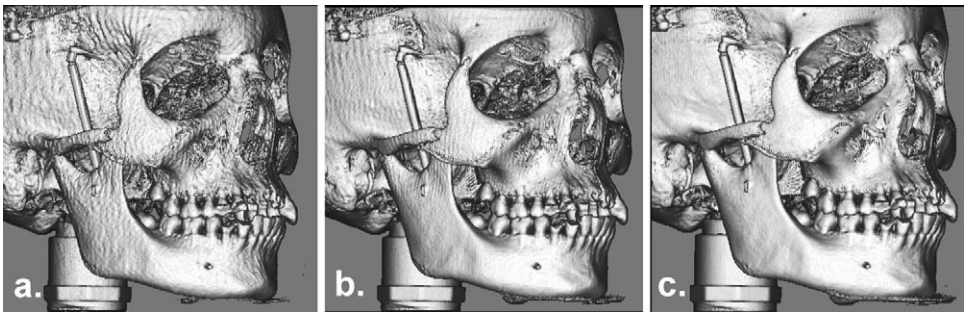

Figure 4. Comparison of 3D shaded surface rendered images from (a) cone beam computed tomography (CBCT) 10. (b) CBCT 20. (c) CBCT 40.

on skulls (mean absolute difference = 0.45 mm ± 0.17 mm) was greater than those obtained from 3D renderings (range: 0.77 mm to 0.88 mm), the latter are consistent with previously reported mean errors of less than 1 mm.[13,15]

For 3D measurements, we found statistical differences between actual and virtual linear measurements for 10 of the 16 dimensions. Relative percentage differences for most were less than 5%. For NC-NC and ANS-PNS, CBCT measurements underestimated actual dimensions by approximately 6% and 10%, respectively. However, for Mo-Mo, CBCT measurements overestimated actual dimensions by 17%. These specific measurement discrepancies may be attributed to interplay of numerous sources of variability. Statistical differences may have resulted from small standard deviations within the measurements. In addition, the greater intraobserver variability demonstrated by the 3D measurements also may have contributed. This is likely because the observer had to identify each landmark on the 3D rendering without the aid of a radiopaque fiducial reference. We believed that this task was a more representative simulation of the clinical situation and provides a combined assessment of inherent 3D landmark definition and identification error as well as error due to imaging procedure.[16] The segmentation process itself was customized for each skull and while not standardized, was adjusted to provide

Table 2. Mean Absolute Error (mm) and Standard Deviation (_SD) of Orthodontic Linear Dimensions for Skulls Compared With Cone Beam Computed Tomography (CBCT) Derived Shaded Surface 3D Renderings Reconstructed From 153 (CBCT 10), 306 (CBCT 20) and 612 (CBCT 40) Basis Projections.

	Modality									
	Skull		CBCT 10		CBCT 20		CBCT 40		Significance	
Measurement	Mean	SD	Mean	SD	Mean	SD	Mean	SD	*F*	*P*
Na-Me[a]	0.44[a]	0.24	0.96[a]	0.48	0.77	0.63	0.87[a]	0.52	7.08	.01
Co-Go (rt)	0.53	0.40	1.19	1.31	0.89	0.60	0.78	0.53	2.17	.13
Co-Go (lt)	0.64	0.60	0.99	0.51	0.88	0.64	0.72	0.54	1.53	.25
Z-Ag (rt)	0.75	0.71	0.81	0.40	0.87	0.50	0.91	0.68	0.24	.87
Z-Ag (lt)[b]	0.40[b]	0.25	0.79[b]	0.37	1.09[b]	0.87	0.92[b]	0.50	8.68	.01
Na-ANS[c]	0.32	0.21	0.58[c]	0.36	0.32[c]	0.21	0.46	0.32	3.43	.042
ANS-PNS[d]	0.71[d]	0.55	1.18[d]	0.50	0.88	0.47	1.00	0.71	3.05	.059
Na-A[e]	0.36[e]	0.32	1.28[e]	1.08	1.05[e]	0.59	1.06[e]	0.36	10.37	<.001
Na-B[f]	0.39[f]	0.23	0.93[f]	0.53	0.80[f]	0.46	0.69[f]	0.39	12.7	<.001
Go-Go	0.48	0.45	0.79	0.50	0.76	0.46	0.68	0.48	2.2	.13
Mf-Mf[g]	0.51[g]	0.32	1.16[g]	0.93	1.29[g]	0.81	0.98[g]	0.51	11.4	<.001
Mo-Mo[h]	0.37[h]	0.32	0.97[h]	0.66	1.33[h]	1.15	0.95[h]	0.37	15.79	<.001
Za-Za[i]	0.10[i]	0.08	0.46[i]	0.25	0.49[i]	0.17	0.52[i]	0.10	27.68	<.001
NC-NC[j]	0.19[j]	0.13	0.63[j]	0.27	0.62[j]	0.28	0.60[j]	0.19	21.49	<.001
Z-Z[k]	0.40[k]	0.22	0.68	0.44	0.56	0.35	0.62[k]	0.29	3.48	.04
J-J	0.57	0.41	0.73	0.42	0.61	0.42	0.57	0.57	0.52	.68
Mean[l]	0.45[l]	0.17	0.88[l]	0.24	0.83[l]	0.28	0.77[l]	0.19	8.24	.14

Modality differences between skull and CBCT measurements:

[a] Skull absolute mean error less than CBCT 10/40 ($P < .001$; $P = .02$).

[b] Skull absolute mean error less than CBCT 10/20/40 ($P = .005$; $P = .024$; $P = .002$).

[c] CBCT 10 greater than CBCT 20 ($P = .024$).

[d] CBCT 10 greater than CBCT 40 ($P = .05$).

[e] Skull absolute mean error less than CBCT 10/20/40 ($P = .01$; $P = .002$; $P = .006$).

[f] Skull absolute mean error less than CBCT 10/20/40 ($P = .001$; $P = .003$; $P = .044$).

[g] Skull absolute mean error less than CBCT 10/20/40 ($P = .02$; $P = .005$; $P = .01$).

[h] Skull absolute mean error less than CBCT 10/20/40 ($P = .025$; $P = .19$; $P = 0$).

[i,j] Skull absolute mean error less than CBCT 10/20/40 ($P < .001$).

[k] Skull absolute mean error less than CBCT 40 ($P = .038$).

[l] Overall skull absolute mean error less than CBCT 10/20/40 ($P < .001$).

optimal ''fill-in'' when the volume was observed from various projections. Finally, it is possible that the landmarks associated with the calculation of these linear dimensions have an inherent error due to landmark identification. While this source of variability and its clinical significance are well acknowledged in 2D cephalometry,[16] the influence of this on 3D cephalometry is, as yet, unreported.

The most clinically important finding of this study was that there was no difference in accuracy between measurements obtained from 3D volumetric renderings, no matter how many projection images were used to create the reconstruction. This is of clinical significance, particularly for CBCT units which use pulsed x-ray generators, because patient exposure will be directly related to the number of projection images acquired. In this study, 3D renderings, produced using 153 basis projection images, provided similar accuracy compared with those produced using 612. This represents a potential patient dose reduction of up to 75% and expels the concept that more is better.

Numerous factors should be considered when applying the results of this investigation to clinical situations. The accuracy of measurement distances between 3D landmarks on actual patients may be affected by a reduction in image quality due to soft tissue attenuation, metallic artifacts, and patient motion. There are also some potential limitations when using 3D images derived from CBCT data. Three-dimensional volumetric depictions depend on appropriate segmentation—the thresholding of bone pixel values and suppression of surrounding tissue values to enhance the structure of interest. This process is dependent on the software algorithm, the spatial and contrast resolution of the scan, the thickness and degree of calcification or cortication of the bony structure, and the technical skill of the operator. In this study, the Dolphin 3D software provides a semi manual method of segmentation, dependent on the interaction of the operator with the data to produce a visually acceptable 3D rendering. These factors may, individually or in combination, result in deficiencies or voids in the surface of the volumetric rendering. These are most likely to occur in regions that are represented by few voxels

Table 3. Mean Length (mm) and Standard Deviation (±SD) of Orthodontic Linear Dimensions for Skulls Compared With CBCT Derived Shaded Surface 3D Renderings Reconstructed From 153 (CBCT 10), 306 (CBCT 20), and 612 (CBCT 40) Basis Projections

		Modality									
		Skull		CBCT 10		CBCT 20		CBCT 40		Significance	
Measurement	Axis	Mean	SD	Mean	SD	Mean	SD	Mean	SD	*F*	*P*
Na-Me[a]	Vertical	109.17[a]	7.34	107.71[a]	7.24	107.65[a]	7.24	107.65[a]	7.28	4.83	.01
Z-Ag (rt)[b]	Vertical	99.88[b]	5.13	94.71[b]	5.85	94.94[b]	5.83	95.11[b]	5.69	9.48	.01
Z-Ag (lt)[c]	Vertical	98.47[c]	4.97	94.92[c]	5.46	94.86[c]	5.65	94.79[c]	5.58	6.37	.01
Co-Go (rt)	Vertical	58.78	4.49	59.88	4.88	59.74	5.11	59.90	5.16	0.78	.52
Co-Go (lt)	Vertical	58.08	4.64	58.36	4.49	58.50	4.82	58.56	4.64	0.55	.66
Na-ANS[d]	Midsagittal	46.29[d]	3.18	45.93	2.99	45.85[d]	3.05	45.84[d]	3.15	2.8	.07
ANS-PNS[e]	Midsagittal	48.84[e]	3.22	43.89[e]	2.88	44.31[e]	3.06	44.2[e]	2.99	86.8	<.001
Na-A	Midsagittal	51.12	3.59	50.69	3.26	50.94	3.97	50.81	3.76	0.88	<.001
Na-B	Midsagittal	89.12	5.85	89.37	6.18	89.44	6.28	89.65	6.49	0.97	.43
Go-Go	Coronal	90.92	8.16	88.37	5.47	88.38	5.57	88.37	5.64	1.27	.32
Mental f-Mental f[f]	Coronal	46.45[f]	3.96	45.67[f]	4.59	45.91	4.5	45.55[f]	3.11	8.96	.01
Mo-Mo[g]	Coronal	19.45[g]	2.16	22.67[g]	1.75	22.89[g]	1.59	22.87[g]	2.13	40.68	<.001
Za-Za[h]	Coronal	121.78[h]	6.13	119.07[h]	5.93	119.03[h]	6.06	119.11[h]	6.09	17.57	<.001
NC–NC[i]	Coronal	24.82[i]	1.52	23.64[i]	1.4	23.39[i]	1.41	23.68[i]	1.46	17.69	<.001
Z-Z[j]	Coronal	94.37[j]	3.28	93.76	3.35	93.69[j]	3.42	93.59[j]	3.37	4.85	.01
J-J	Coronal	60.94	2.93	60.86	3.27	60.63	3.20	60.82	3.16	1.97	.16

Modality differences between skull and CBCT measurements:
[a] Skull dimensions greater than CBCT 10/20/40 ($P = .006$; $P = .006$; $P = .005$).
[b,e,h] Skull dimensions greater than CBCT 10/20/40 ($P < .001$).
[c] Skull dimensions greater than CBCT 10/20/40 ($P = .002$; $P = .001$; $P = .001$).
[d] Skull dimensions greater than CBCT 20/40 ($P = .044$; $P = .047$).
[f] Skull dimensions greater than CBCT 10/40 ($P = .05$; $P = 0$).
[g] Skull dimensions less than CBCT 10/20/40 ($P < .001$).
[i] Skull dimensions greater than CBCT 10/20/40 ($P = .002$; $P < .001$; $P < .001$).
[j] Skull dimensions greater than CBCT 20/40 ($P = .02$; $P = .01$).

or have gray values still representing bone, but outside the threshold. These areas include the posterior and anterior superior walls of the maxillary sinus, bone overlying the roots of the teeth and cortical bone of the mandibular condyle. Consequently, this may lead to greater landmark identification error and subsequent measurement error.

Anatomic landmarks used in this study whose accuracy may be affected by poor segmentation include Mo, A point, ANS, PNS, and Mf. In addition, the method of establishing dimensional truth could have potentially contributed to bias in the results. While the landmark identification and measurements on the 3D rendered images were repeated three times by a single observer, the landmark identification on the skulls was performed only once and measurements performed independently three times by consensus of two observers. This reduced the error of point identification on the skulls; however, the establishment of a consensus landmark location was necessary to provide a fiducial reference to which we could assess the inherent clinical inaccuracies of both landmark identification and measurement associated with the 3D image rendering.

Based on the comparable accuracy of dimensions obtained from 3D rendered images reconstructed using the lowest number of projection images, it is unwise to interpret the findings of this study as advocating the use of CBCT in general orthodontic practice. Our study does not take into account the overall comparative radiation detriment required to produce such images nor the clinical efficacy of the technique compared to conventional imaging. However, we do advocate clinical cost/benefit analyses incorporating exposure considerations to assist in developing appropriate patient selection criteria for the use of CBCT in cephalometric imaging.

CONCLUSIONS

- Linear measurements on 3D shaded surface renderings from CBCT datasets using commercial cephalometric analysis software have variable accuracy.
- Reducing the number of image projections needed to construct a 3D shaded surface rendering does not result in reduced dimensional accuracy of 3D measurements and potentially provides reduced patient radiation exposure.

ACKNOWLEDGMENT

The authors wish to thank Dr Mazar Moshiri, Department of Orthodontics and Pediatric Dentistry, University of Louisville

School of Dentistry for his contribution to the data collection stage of this research.

REFERENCES

1. Hilgers ML, Scarfe WC, Scheetz JP, Farman AG. Accuracy of linear TMJ measurements with cone beam computed tomography and digital cephalometric radiography. *Am J Orthod Dentofacial Orthop.* 2005;1278:803–811.
2. Farman AG, Scarfe WC. Development of imaging selection criteria and procedures should precede cephalometric assessment with cone-beam computed tomography. *Am J Orthod Dentofacial Orthop.* 2006;130:257–265.
3. Moshiri M, Scarfe WC, Hilgers ML, Scheetz JP, Silveira AM, Farman AG. Accuracy of linear measurements from imaging plate and lateral cephalometric images derived from cone-beam computed tomography. *Am J Orthod Dentofacial Orthop.* 2007;132:550–560.
4. Kumar V, Ludlow JB, Mol A, Cevidanes L. Comparison of conventional and cone beam CT synthesized cephalograms. *Dentomaxillofac Radiol.* 2007;36:263–269.
5. Lagravère MO, Hansen L, Harzer W, Major PW. Plane orientation for standardization in 3-dimensional cephalometric analysis with computerized tomography imaging. *Am J Orthod Dentofacial Orthop.* 2006;129:601–604.
6. Lagravère MO, Major PW. Proposed reference point for 3-dimensional cephalometric analysis with cone-beam computerized tomography. *Am J Orthod Dentofacial Orthop.* 2005;128:657–660.
7. Hashimoto K, Arai Y, Iwai K, Araki M, Kawashima S, Terakado M. A comparison of a new limited cone beam computed tomography machine for dental use with a multidetector row helical CT machine. *Oral Surg Oral Med Oral Pathol Oral Radiol Endod.* 2003;95:371–377.
8. Schulze D, Heiland M, Thurmann H, Adam G. Radiation exposure during midfacial imaging using 4- and 16-slice computed tomography, cone beam computed tomography systems and conventional radiography. *Dentomaxillofac Radiol.* 2004;33:83–86.
9. Ludlow JB, Davies-Ludlow LE, Brooks SL. Dosimetry of two extraoral direct digital imaging devices: NewTom cone beam CT and Orthophos Plus DS panoramic unit. *Dentomaxillofac Radiol.* 2003;32:229–243.
10. Ludlow JB, Davies-Ludlow LE, Brooks SL, Howerton WB. Dosimetry of 3 CBCT devices for oral and maxillofacial radiology: CB Mercuray, NewTom 3G and i-CAT. *Dentomaxillofac Radiol.* 2006;35:219–226.
11. Tsiklakis K, Donta C, Gavala S, Karayianni K, Kamenopoulou V, Hourdakis CJ. Dose reduction in maxillofacial imaging using low dose Cone Beam CT. *Eur J Radiol.* 2005;56:413–417.
12. Swennen GR, Schutyser F. Three-dimensional cephalometry: spiral multi-slice vs cone-beam computed tomography. *Am J Orthod Dentofacial Orthop.* 2006;130:410–416.
13. Cavalcanti MGP, Haller JW, Vannier MW. Three-dimensional computed tomography landmark measurement in craniofacial surgical planning: experimental validation in vitro. *J Oral Maxillofac Surg.* 1999;57:690–694.
14. Kusnoto B, Evans CA, BeGole EA, De Rijk W. Assessment of 3-dimensional computer-generated cephalometric measurements. *Am J Orthod Dentofacial Orthop.* 1999;116:390–399.
15. Kragskov J, Bosch C, Gyldensted C, Sindet-Pedersen S. Comparison of the reliability of craniofacial anatomic landmarks based on cephalometric radiographs and three-dimensional CT scans. *Cleft Palate Craniofac J.* 1997;34:111–116.
16. Kamoen A, Dermaut L, Verbeeck R. The clinical significance of error measurement in the interpretation of treatment results. *Eur J Orthod.* 2001;23:569–578.